Basis for the phototaxis sign reversal in the green alga *Chlamydomonas reinhardtii* studied by high-speed observation

Masako Nakajima[1,2†] Kosuke Iizuka[3†], Rina Takahashi[1,4], Noriko Ueki[5], Atsuko Isu[1], Kenjiro Yoshimura[6], Toshiyuki Nakagaki[3], Toru Hisabori[1,2,4], Katsuhiko Sato[3*], and Ken-ichi Wakabayashi[1,2,4*]

1: Laboratory for Chemistry and Life Science, Institute of Innovative Research, Tokyo Institute of Technology, Yokohama, 226-8503 Japan

2: Department of Environmental Chemistry and Engineering, Interdisciplinary Graduate School of Science and Engineering, Tokyo Institute of Technology, Yokohama, 226-8503 Japan

3: Research Institute for Electronic Science (RIES), Hokkaido University, Sapporo 001-0020, Japan

4: School of Life Science and Technology, Tokyo Institute of Technology, Yokohama, 226-8503 Japan

5: Science Research Center, Hosei University, 2-17-1 Fujimi, Chiyoda-ku, Tokyo 102-8160, Japan

6: Department of Machinery and Control Systems, College of Systems Engineering and Science, Shibaura Institute of Technology, Saitama 337-8570, Japan

†: These authors contributed equally to this work.

*: To whom correspondence should be addressed: KW, wakaba@res.titech.ac.jp; KS, katsuhiko_sato@es.hokudai.ac.jp

ABSTRACT

For organisms that respond to environmental stimuli using taxes, reversal of the tactic sign should be tightly regulated for survival. The biciliate green alga *Chlamydomonas reinhardtii* is an excellent model for studying reversal between positive and negative phototaxis. *C. reinhardtii* cells change swimming direction by modulating the balance of beating forces between their two cilia after photoreception at the eyespot; however, it remains unknown how they reverse phototactic sign. In this study, we observed cells undergoing phototactic turns with a high-speed camera and found that two key factors determine the phototactic sign: which of the two cilia beats more strongly for phototactic turning and when the strong beating starts. The timing of the strong ciliary beating is suggested to be regulated by ROS-regulated switching between the light-on and light-off responses at the eyespot, which leads to the switching between positive and negative phototaxis. This idea is supported by a mathematical model that introduces the timing of the strong ciliary beating after photoreception.

Keywords:

Chlamydomonas reinhardtii, phototaxis, flagella/cilia, ROS, mathematical model

43 **INTRODUCTION**

44 The biciliate unicellular green alga *Chlamydomonas reinhardtii* is an excellent model
45 organism to study how organisms respond to changing light conditions. *C. reinhardtii*
46 shows a distinct light-induced behavior known as phototaxis, in which cells swim either
47 toward or away from a light source (called positive or negative phototaxis,
48 respectively). The direction of phototaxis, referred to here as the sign (either positive or
49 negative), can be reversed. The regulation of this sign reversal is thought to be
50 important for the viability of photosynthetic algae, but its mechanism is not well
51 understood.

52 In *C. reinhardtii*, the light signal for phototaxis is received by the eyespot
53 (Foster & Smyth, 1980), an organelle that appears under a microscope as an orange spot
54 near the cell equator. It consists of carotenoid-rich granule layers, and a small area of
55 plasma membrane in which channelrhodopsin (ChR) molecules are localized (Fig. 1A).
56 The carotenoid-rich granule layers (CLs) function as a quarter-wave plate that reflects
57 light (Foster & Smyth, 1980; Ueki et al., 2016), while ChR molecules are light-gated
58 ion channels (Nagel et al., 2002; Nagel et al., 2003; Sineshchekov, Jung, & Spudich,
59 2002; Suzuki et al., 2003). Because of the relative position of these two components, the
60 eyespot perceives light with high directionality. When a light signal arrives from the

61 ChR-facing side, the light signal is amplified by reflection from the CLs; conversely,
62 light signals are blocked by the CLs when coming from the CL-facing direction. In
63 addition, while swimming, the cell rotates around its anterior-posterior axis. Directional
64 photoreception by cells that swim with bodily rotation enables them to accurately detect
65 and move in the direction of light stimuli.

66 Previous studies suggest that the phototaxis pathway in *C. reinhardtii* consists
67 of three steps: 1) photoreception by ChRs, 2) an increase in intraciliary [Ca^{2+}], and 3) a
68 change in the balance of beating between the two cilia (a.k.a. flagella). After
69 photoreception, the forces generated by the two cilia of *C. reinhardtii* become
70 imbalanced, changing the cell's swimming direction. These two cilia can be
71 distinguished by their position relative to the eyespot, with the one nearest the eyespot
72 called the *cis*-cilium, and the other called the *trans*-cilium. A currently prevailing model
73 explains the mechanism underlying positive phototaxis as follows: When the eyespot
74 faces a light source during swimming with bodily rotation, ChRs open to allow for Ca^{2+}
75 entry, intraciliary [Ca^{2+}] increases, and the *trans*-cilium starts to beat more strongly than
76 the *cis*-cilium, by increasing beating amplitude and/or frequency (Kamiya & Witman,
77 1984; Rüffer & Nultsch, 1991). The imbalance between the forces generated by the two
78 cilia tilts the cell's swimming direction toward the eyespot-bearing side (i.e., in the

79 direction of the light source). After 180º of rotation, the eyespot stops receiving light
80 due to the shielding of CLs, the ChRs close, intraciliary [Ca^{2+}] decreases due to some
81 ion pumping activity, and the force generated by the *cis*-cilium increases while that of
82 the *trans*-cilium decreases, resulting in the cell's swimming direction tilting toward the
83 light-source. By repeating this process, the cell will swim toward the light source,
84 displaying positive phototaxis (Fig. 1B). However, in contrast to this widespread model,
85 phototactic turns may also be initiated when the eyespot faces away from the light
86 source (i.e., when the eyespot is shaded) (Isogai, Kamiya, & Yoshimura, 2000).
87 How, then, can the sign of phototaxis be reversed? Two possibilities exist: (i)
88 The *cis*-cilium, rather than the *trans*-cilium, beats more strongly when $[Ca^{2+}]_i$ increases
89 upon photoreception (referred to as "the dominant arm model"); and (ii) after
90 photoreception, the *trans*-cilium beats more strongly than the *cis*-cilium when the cell
91 makes a half bodily rotation and the eyespot faces the opposite side to the light source
92 (referred to as "the off-response model). These possibilities should be verified by
93 observing cell behavior after inducing positive or negative phototaxis.
94 Several factors are known to induce sign-switching of phototaxis in *C.*
95 *reinhardtii*, including light intensity (Feinleib & Curry, 1971), extracellular Ca^{2+}
96 concentration (Morel-Laurens, 1987), circadian rhythms (Kondo, Johnson, & Hastings,

97 1991), photosynthetic activities (Takahashi & Watanabe, 1993). Of these factors, the
98 amount of cellular reactive oxygen species (ROS) changes the sign of phototaxis most
99 intensely (Wakabayashi et al., 2011). Applying membrane-permeable ROS reagents or
100 membrane-permeable ROS scavengers to cells can strongly bias the phototactic sign to
101 positive or negative, respectively.

102 In this study, to test the two possibilities (i) and (ii) above, we carried out
103 high-speed observations of cells turning during positive or negative phototaxis, after
104 treatment with either a membrane-permeable ROS or a membrane-permeable ROS
105 scavenger. Our results showed that the both (i) and (ii) are the cases. The innate
106 phototactic sign of a strain can be explained by the case (i): after photoreception, we
107 observed that positively phototactic strain cells beat the *trans*-cilium more strongly,
108 whereas negatively phototactic strain cells beat the *cis*-cilium more strongly. When the
109 same strain reverses the phototactic signs, the case (ii) applies: for example, the
110 positively phototactic strain cells showed negative phototaxis by beating the trans-
111 cilium more strongly when the eyespot faced opposite to the light source. The case (ii)
112 can be interpreted in two ways: (a) the strong beating was induced by a light-off
113 response of the eyespot, or (b) the light-on response of the eyespot was delayed by the
114 time it takes for the cell to make a half rotation. We developed a mathematical model

that satisfies the cases (i) and (ii). The model strongly suggested that the case (a) would be the case, which was confirmed by additional experiments using the slow-swimming cells.

119 **RESULTS**

120 **Two hypotheses to explain the sign change of phototaxis**

121 The mechanism underlying positive phototaxis can be explained as described in the
122 Introduction (shown in Fig. 1B). To elucidate the mechanism of negative phototaxis, we
123 considered two models (Fig. 1C), in which the dominant cilium is a key factor (defined
124 here as the cilium that begins to beat more strongly after photoreception than the other).
125 In the first model (the dominant-arm model), we assume that the relationship between
126 the dominant cilium and $[Ca^{2+}]_i$ is reversed, such that the *cis*-cilium, rather than the
127 *trans*-cilium, becomes dominant when $[Ca^{2+}]_i$ is increased. If the *cis*-cilium beats more
128 strongly than the *trans*-cilium after light perception (which elicits Ca^{2+} influx), the cell
129 will undergo negative phototaxis. In the second model (the off-response model), we
130 assume that the relationship between the dominant cilium and $[Ca^{2+}]_i$ remains the same,
131 but the onset of ciliary dominance (along with $[Ca^{2+}]_i$ increase) occurs when the eyespot
132 faces away from the light source, and senses a light-off stimulus. In this case, the cell
133 will also show negative phototaxis.

134

135 **Dominant cilium differs in strains with opposite phototactic signs**

136 To determine which of these two models was more plausible, we observed the turning
137 of *C. reinhardtii* cells using a high-speed camera (150 fps) linked to green light-
138 emitting diode (LED) illumination sources at right angles. This system was an extension
139 of the right-angle illumination system originally designed for the previous study (Isogai
140 et al., 2000), which we here improved upon to observe the phototactic turnings and the
141 eyespot position simultaneously by synchronizing the high-speed camera and the LED
142 illumination. This allowed us to determine the exact time when a light stimulus was
143 applied to a rotating cell, and the simultaneous orientation of the eyespot (visible as a
144 bright spot under a dark-field microscope with an oil-immersion condenser). With this
145 system, we first induced phototaxis in cells using the weaker stimulus of Light 1 (Fig.
146 2A). Then, the stronger Light 2 was illuminated at right angles to Light 1. When the
147 eyespot in a swimming cell faced the light-source side of Light 2 (or the light side) after
148 its illumination, we considered the cell to have perceived the light in that time frame
149 (Fig. 2A). Then, from the position of the eyespot and the swimming path, we assessed
150 which cilium beat more strongly (SI Movies S1-S4).
151 We observed the eyespot position during phototactic turning in two genetically
152 different strains, CC-124 (a negatively phototactic strain, here referred to as NP) and
153 CC-125 (positively phototactic strain, PP) (see Materials and Methods). We analyzed

154 only those cells that showed phototactic turnings of one full self-rotation after
155 photoreception. We found that PP cells usually showed positive phototaxis. Similar to
156 the PP cell after treatment with *t*-BOOH that induces positive phototaxis in Fig. 2A, a
157 typical control PP cell changed its swimming direction immediately after it detected
158 Light 2 (green arrow position). When turning toward the direction of the light source,
159 more than half of the cells performed phototactic turning while the eyespot was located
160 on the light side (i.e., the *trans*-cilium became dominant immediately after
161 photoreception) (Fig. 2B).

162 In contrast, NP cells usually showed negative phototaxis. Similar to the NP cell
163 after treatment with DMTU that induces negative phototaxis in Fig. 2A, a typical
164 control NP cell changed its swimming direction immediately after it detected Light 2,
165 similar to the PP cell. When turning against the direction of the light source, most cells
166 performed turns while the eyespot was located on the light side, i.e. the *cis*-cilium
167 became dominant immediately after photoreception (Fig. 2B). These observations
168 suggest that the difference between PP and NP cells can be explained by the "Dominant
169 arm model." The cilium that becomes dominant after photoreception is genetically
170 determined. Therefore, if the dominant cilium is the *trans*-cilium, the strain tends to

171 show positive phototaxis, while if it is the *cis*-cilium in another strain, it tends to show

172 negative phototaxis.

173

174 **Reversal of phototactic sign by "off-response" of the dominant cilium**

175 Next, we examined the effect of reagents that change the cellular ROS, affecting the

176 phototactic sign. After treatment with 0.2 mM *t*-BOOH, a membrane-permeable ROS

177 reagent that induces positive phototaxis in both strains, most PP cells made phototactic

178 turns while the eyespot was located on the light side, while most NP cells made

179 phototactic turns while the eyespot was located on the dark side (i.e., the side opposite

180 the light-source) (Fig. 2B) (SI Movie S1, S2). Fig. 2A shows the representative data,

181 and the *t*-BOOH-treated NP cell changed its swimming direction after the cell made a

182 half-self-rotation (magenta arrow). In contrast, after treatment with 75 mM DMTU, a

183 membrane-permeable ROS scavenger that induces negative phototaxis in both strains,

184 most PP cells made phototactic turns while the eyespot was located on the dark side,

185 and most NP cells made phototactic turns while the eyespot was located on the light

186 side (SI Movie S3, S4). In Fig. 2A, the DMTU-treated PP cell changed its swimming

187 direction after the cell made a half-self-rotation (magenta arrow).

188 Thus, the sign-reversal of phototaxis in both strains can be explained by the
189 off-response model; i.e., *t*-BOOH induces the onset of *cis*-cilium dominance in the dark
190 side in NP cells and DMTU induces that of *trans*-cilium dominance in the light side in
191 PP cells. Simply put, the reversal of genetically determined phototactic signs in a given
192 strain is achieved by reversing the eyespot position relative to the light source (the light
193 or dark side) when its genetically determined dominant cilium starts to show stronger
194 beating than the other after light stimulation. We found that the dominant cilium after
195 photoreception of PP cells was always the *trans*-cilium, while that of NP was always
196 the *cis*-cilium. In each strain, the sign-switching of phototaxis was caused by the onset
197 of strong beating of the dominant cilium on the dark side.
198 Therefore, these phototactic turning events can be categorized into two cases
199 for each sign of phototaxis. For cells displaying positive phototaxis: in (Positive Case
200 1), phototactic turning occurred while the eyespot was located on the light side. In this
201 case, the *trans*-cilium must have become dominant in response to the light-on stimulus
202 (such as PP cells without the ROS-reagents or with *t*-BOOH). In (Positive Case 2),
203 phototactic turning occurred while the eyespot was located on the dark side. In this case,
204 the *cis*-cilium must have become dominant in response to the light-off stimulus (such as
205 NP cells with *t*-BOOH). For cells displaying negative phototaxis: in (Negative Case 1),

206 phototactic turning occurred while the eyespot was located on the light side. In this
207 case, the *cis*-cilium must have become dominant in response to the light-on stimulus
208 (such as NP cells without the ROS-reagents or with DMTU). In (Negative Case 2),
209 phototactic turning occurred while the eyespot was located on the dark side. In this case,
210 the *trans*-cilium must have become dominant in response to the light-off stimulus (such
211 as PP cells with DMTU).
212
213 **Eyespot position in the helical paths**
214 Regarding changes in the balance of beating between the two cilia during phototactic
215 turning, we first wanted to examine the force balance in unstimulated cells. Under
216 homogeneous light conditions, *C. reinhardtii* cells swim in a helical path, due to the
217 imbalanced force generation of the two cilia beating in slightly skewed planes (Fig.
218 S1A). In previous work, Isogai et al. showed that the eyespot is located on the outer
219 edge of the helical swimming paths in ~80 percent of positively phototactic cells (Isogai
220 et al., 2000). In contrast, for negatively phototactic cells, ~50 percent of cells swim with
221 the eyespot facing inside, whereas ~30 percent of cells swim with the eyespot facing
222 outside (Isogai et al., 2000). These results suggest that eyespot position in the helical
223 swimming path is partially correlated with the phototactic sign, but the correlation is not

224 determinative. We thus investigated whether the eyespot position in the swimming
225 paths is affected by ROS-modulating reagents. Most, but not all, cells swam with the
226 eyespot outside the helix when they showed either positive phototaxis (Fig. S1B, Sign
227 P). However, when cells showed negative phototaxis in the presence of DMTU,
228 directing the eyespot inside the helix was observed almost as frequently as towards the
229 outside (Fig. S1B, Sign N, +DMTU). Thus, we did not observe a strict correlation either
230 between phototactic sign and eyespot position in the helical paths.

231 To elucidate if the dominant cilium after photoreception is also dominant in the
232 swimming without light stimulation, we observed the PP and NP cells swimming under
233 a microscope in the red background light. The results showed that ~60% cells swam
234 with the eyespot facing outward of the helical path and the rest swam with it inward in
235 both PP and NP cells (Fig. S1C). These data also suggest that the dominant cilium after
236 photoreception is independent from that without photostimulation. These results are
237 consistent with those of a mathematical model that describes the swimming behavior of
238 *C. reinhardtii* given in the section of "Mathematical model to test the experimental
239 data," which shows that whether the eyespot faces outward or inward of the helical path
240 does not affect the sign of phototaxis.

241

242 **Photoreceptor currents after treatment with the ROS-modulating reagents**

243 A possible explanation for how ROS-modulating reagents induce the light-off response
244 is that those reagents delay the response of the dominant cilium by slowing the opening
245 of photo-gated channels (ChRs). If this delay is as long as the time required for a cell to
246 perform a half rotation (~250 msec), then the phototactic sign of the cell would reverse.
247 To test this possibility, we measured the photoreceptor current (PRC) in a population of
248 *C. reinhardtii* cells by the method of Sineshchekov et al. (Sineshchekov et al., 1992;
249 Sineshchekov et al., 1994) (Fig. S2A). Treatment with *t*-BOOH did not significantly
250 affect the magnitude of PRC produced by a single flash of light stimulation, in either PP
251 or NP cells (Fig. S2B, C). We also measured the time (delay) required for the
252 generation of PRC after photostimulation, but detected no significant difference
253 between the control and the *t*-BOOH-treated cells (Fig. S2B, C). In contrast, after
254 treatment with DMTU, we found that PRC decreased, while delay time increased, in
255 both strains (Fig. S2B, C). However, the increase in delay time was only ~1 msec.
256 These results suggest that the light-off response is not caused by the delay in PRC
257 generation.

258

259 **Mathematical model to test the experimental data**

We have shown that there are two cases where the phototactic sign of *C. reinhardtii* is reversed: (i) dominant arm model case and (ii) off-response model case. In the off-response model case, however, there is another interpretation of the experimental results, namely, if *C. reinhardtii* has a time delay for the response to the light stimulus and the delay time is so long that the cell rotates half a turn about its anterior-posterior axis, the phototactic turning occurs when the eyespot faces on the dark region; we refer to this hypothesis as "the time delay model". To examine whether the time delay changes the phototactic sign of the cell and determine whether the off-response model or the time delay model is more plausible for explaining phototactic turning when the eyespot facing on the dark side, we develop a mathematical model that express the time delay of the cell. Our modeling framework is based on previous models of phototaxis in *C. reinhardtii* and the multicellular green alga *Volvox carteri* (Bennett & Golestanian, 2015; Drescher, Goldstein, & Tuval, 2010, Leptos et al., 2018). We extend them by explicitly introducing a time delay into the ciliary response after a light stimulus (see SI Appendix A for details). Brief description of our mathematical model is below.

We approximate the cell as a rigid ball and define the body axes of the cell as in Fig. 3A, where **a, b** and **c** are unit vectors that are fixed to the body of the cell. We assume

that a cell swims with cilia forward, with a constant speed v_0 in the posterior direction $\mathbf{c}$, i.e., $\mathbf{v} = v_0\mathbf{c}$, and rotates with the angular velocity

$$\boldsymbol{\omega}(t) = -\omega_c^{(0)}\,\mathbf{c} + (\omega_a^{(0)} - p(t))\mathbf{a}, \quad \text{——[1]}$$

where $\omega_c^{(0)}$ and $\omega_a^{(0)}$ are constants, which represent the proper angular velocity of the cell under unstimulated conditions. The quantity p expresses the contribution from the change in the behaviors of the two cilia in response to the change in light intensity at the eyespot: when the *trans*-cilium beats stronger than the *cis*-cilium, p becomes positive, and vice versa. We assume that the response of dominant cilium to the light stimulus has some constant delay. Indeed, under the normal culture conditions the response of dominant cilium to the light has a short delay time around 30-40 msec (Rüffer & Nultsch, 1991; Witman, 1993). We extend this notion and allow the delay time τ_0 to be any. We thus write the relationship between p and light intensity received by the eyespot, I, as

$$p(t) = \gamma_0 \frac{dI(t-\tau_0)}{dt}, \quad \text{——[2]}$$

where γ_0 is a constant that takes the value +1 or -1. $\gamma_0 = +1$ means the *trans*-cilium is dominant (as in PP), while $\gamma_0 = -1$ means the *cis*-cilium is dominant (as in NP). By changing the value of γ_0, we express the dominant arm model. τ_0 is the delay time of the onset of the ciliary dominance after photoreception. By changing the value of τ_0 we can investigate the effects of the time delay of dominant cilium to light stimulus on phototaxis. In the mathematical description, the light-off response model in fact coincides with the dominant arm model, because the onset of dominant cilium at step-

down stimulus ($\gamma_0 = +1$ and $dI/dt < 0$) and the onset of exchanged dominant cilium at step-up stimulus ($\gamma_0 = -1$ and $dI/dt > 0$) cannot be distinguished in this framework. Thus this model is used to compare the results of the time delay model and those of the other models, dominant arm model and off-response model.

The light intensity *I* received by the eyespot is given by $I(t) = I_0(-\mathbf{e}_{light} \cdot \mathbf{e}_{eyespot} + 1)/2$, where I_0 is the intensity of the light at the cell position. $\mathbf{e}_{light}$ and $\mathbf{e}_{eyespot} = (\mathbf{a} + \mathbf{b})/\sqrt{2}$ are unit vectors that represent the direction of the incident light and the eyespot, respectively. The time evolution equations for this model are closed in terms of the Euler angles $(\theta_1, \theta_2, \theta_3)$ that specify the directions of body axes, **a**, **b**, **c** (Fig. 3B) (Landau, 1976) and the position of the cell $\mathbf{r} = (x, y, z)$.

With this model we consider a simple situation where a parallel light comes from the positive z direction (Fig. 3B), which is expressed by $\mathbf{e}_{light} = (0, 0, -1)$ and constant I_0. If the cell goes in the positive z direction in the final state, this situation indicates positive phototaxis, while if the cell goes in the negative z direction in the final state, that is negative phototaxis.

This mathematical model in fact has two steady solutions (Eqs. S5 and S6 in Appendix B) for any parameters: one represents positive phototaxis, where the cell swims in the positive z direction with a constant speed, drawing a left-handed spiral trajectory. The other represents negative phototaxis, where the cell swims in the negative z direction with the same speed, drawing a left-handed spiral trajectory. Thus the model intrinsically involves both positive and negative phototaxis states. Depending on the values of model parameters, γ_0, I_0 and τ_0, in the relation between p and I, the

stability of the two steady solutions changes (Fig. S3), and one stationary solution is selected (Fig. 3C, D; SI Movies S5,S6). The stability of the steady solutions does not depend on v_0, because the time evolution equations for $(\theta_1, \theta_2, \theta_3)$ that spesify the direction of the cell are closed in terms of $(\theta_1, \theta_2, \theta_3)$ only (see Eq. S4 in Appendix A) and do not contain v_0.

Furthermore, from the steady solutions of this model we find the relationships between the parameters involved in our mathematical model ($\omega_a^{(0)}$, $\omega_c^{(0)}$, v_0) and the quantities concerning the helical path of the cell observed in experiments as

$$\omega_a^{(0)} = \pm \frac{4\pi^2 H^2 r_0}{\sqrt{v_z^{\,2} + 4\pi^2 H^2 r_0^{\,2}}}$$

$$\omega_c^{(0)} = \frac{2\pi H \,|\, v_z \,|}{\sqrt{v_z^{\,2} + 4\pi^2 H^2 r_0^{\,2}}} \quad \text{, ---[3]}$$

$$v_0 = \sqrt{v_z^{\,2} + 4\pi^2 H^2 r_0^{\,2}}$$

where r_0, H and $|\, v_z \,|$ are the radius, Heltz, and speed of the cell along the axis of helical path drawn by the cell under homogeneous light conditions, respectively (see Appendix C for deitals). Using eq. 3 we can determine the values of model parameters $\omega_a^{(0)}$, $\omega_c^{(0)}$, v_0 from experimental data, except for the sign of $\omega_a^{(0)}$. (Note that the first relation in Eq. 3 has plus minus sign.) The sign of $\omega_a^{(0)}$ is in fact related to the relative position of the eyespot in the helical orbit of the cell (Appendix C), i.e., when $\omega_a^{(0)} > 0$ the eyespot face the outside of the helical orbit, while when $\omega_a^{(0)} < 0$ the eyespot faces the inside of helical orbit. This result holds independent of phototactic sign. That is, for each phototaxis, there are two cases where the eyespot faces the outside and inside of the helical path. In which direction the eyespot faces is determined by only the sign of

$\omega_a^{(0)}$. Using this property we can also determine the sign of $\omega_a^{(0)}$ from the position of eyespot in the helical path. Most cells observed in our experiments exhibit that the relative position of eyespot to the helical orbit is the outside, so we take $\omega_a^{(0)} > 0$ throughout this model. Hence the control parameters of this model turn out to be γ_0, I_0 and τ_0.

To check whether this mathematical model exhibits definite phototaxis for given parameters, we numerically integrated the time evolution equations Eqs. S3 and S4 in Appendix A with some initial conditions with the Euler methd ($\Delta t = 1/10000$). Figure 3 C,D give the trajectories of the cell described in our model for $\tau_0 = 0.08$ (C) and $\tau_0 = 0.34$ (D). We see that in Fig. 3C the cell goes in the positive z direction in the final state (positive pototaxis), while in Fig. 3D, the cell goes in the positive z direction (negative pototaxis). These final swimming directions do not depend on the initial conditions, i.e., even if the cell directed in any direction at the initial time, the final swimming direction (positive or negative phototaxis) is determined only by the values of the model parameters, I_0, γ_0 and τ_0. To see how the swimming direction depends on the model parameters, we drew the phase diagram of the final velocity of the cell (Fig. 4), where the values of $\omega_c^{(0)}$, $\omega_a^{(0)}$ and v_0 used here were obtained from experimental data on the PP cell using the relations Eq. 3. In Fig. 4 we see that when γ_0 is changed from +1 to -1, the swimming direction of the cell becomes opposite. This means that when the dominant cilium is exchanged, the phototactic sign is reversed. This result is consistent with our experimental data in section _ and also with the existing works [interface, Bennett & Golestanian, 2015, PRL]. Whenever the sign of

γ_0 is changed, the phototactic sign is also changed, which comes from the symmetry of the mathematical model.

When we fix the values of I_0 and γ_0 and change only τ_0, the final swimming direction also changes (Fig. 4). For example, let us see the case of $I_0 = 0.1$ and $\gamma_0 = +1$ in Fig. 4. In this case photatctic sign becomes plus when $0.06 < \tau_0 < 0.3$ [sec], and the phototactic sign becomes minus when $0.3 < \tau_0 < 0.4$ [sec]. Since the mean self-rotation frequency of the PP cell about the anterior-posterior (AP) axis in experiments is about 2 Hz (see Table 1), the time needed for the cell to rotate about the AP axis one-half is about 0.25 [sec]. Thus, the above results of numerical simulations are basically consistent with the picture of the time delay model, i.e., we can consider that for $0 < \tau_0 < 0.25$ the eyespot faces on the bright side, while for $0.25 < \tau_0 < 0.5$ the eyespot faces on the dark side. That is, there is a possibility that the behaviors of the cells obaserved in experiments given in section may be the result of delayed response of the cell to the light stimulus.

Off-response or delayed response?

In the Off-response model, ciliary dominance starts to occur on the dark side. We interpreted this as an immediate response to a light-off signal. However, it may also be a delayed response to a light-on signal. If the delay time τ_0 is fixed between 0.25 sec and 0.5 sec, a delayed response to a light-on stimulus would just look like a light-off

381 response without a delay. To assess which of these two interpretations is more
382 plausible, we conducted two experiments and a simulation.
383 First, we observed phototaxis in slow-swimming mutants *ida4* (lacking inner-
384 arm dynein subspecies a, c and d) and *oda1* (lacking entire outer-arm dynein) after
385 treatment with ROS-modulating reagents (Kamiya, 1988; Kamiya et al., 1991; Takada
386 et al., 2002). As the bodily rotation of the cell is caused by the slightly three-
387 dimensional beating of the two cilia, slow-swimming mutants show bodily rotation with
388 a longer rotation cycle time, as we observed (Table 1). If the delay time is between 0.25
389 and 0.50 sec, those slow-swimming mutants may differ in phototactic sign from the
390 wild-type PP and NP strains. We found that both *oda1* and *ida4* cells tended to display
391 positive phototaxis under neutral or oxidizing conditions, and negative phototaxis under
392 reducing conditions, similarly to the PP strain of the wild type (Fig. 5A, B). However,
393 the sign-reversal in the slow-swimming mutants was not as clear as in the wild type,
394 especially after treatment with the ROS-scavenger. It is possible that the force
395 generation for steering is weaker under these conditions in the slow-swimming mutants.
396 Thus, we also observed phototaxis of PP cells after treatment with DMTU in a
397 viscous medium. If the negative phototaxis of PP cells is achieved by the delayed
398 response, the DMTU-treated PP cells may not be able to show negative phototaxis when

399 the self-rotation duration is prolonged. In the medium containing 4.5% or 9.0%
400 Ficoll400, cells swam slowly (Table 2). Even in these media, the DMTU-treated PP
401 cells showed clear negative phototaxis (Fig. 6). These results cannot be achieved by the
402 delayed response.

403 We also used our mathematical model to simulate the behavior of cells that
404 self-rotate at a lower-than-normal frequency of 1.25 Hz and 0.72 Hz, frequencies of
405 *ida4* and *oda1*, respectively (Table 1). Our simulation results indicated that when τ_0 is
406 between 0.075 and 0.5 sec (when self-rotation frequency is 1.25 Hz) or 0.25 and 0.5 sec
407 (0.72 Hz), such cells do not change phototactic signs with a change in τ_0, unlike the
408 wild type cells that rotate at higher frequencies of ~2 Hz (Fig. 7). Furthermore, we
409 carried out similar simulations using the self-rotation frequency of cells in viscous
410 media (Table 2). In a medium containing 9.0% Ficoll400, the rotation frequency is
411 ~0.91 Hz (Table 2). In this case, when τ_0 is between 0.15 and 0.7 sec, cells do not
412 change phototactic signs with a change in τ_0 unlike cells in a regular medium (Fig. S4).

413 Considering the above three results together, it is more likely that the onset of
414 ciliary dominance alteration on the dark side takes place in direct response to a light-off
415 stimulus, rather than as a delayed response to a light-on stimulus.

416

417 **DISCUSSION**

418 In this study, we observed initial phototactic turning of *C. reinhardtii* cells after
419 photostimulation with high-speed video recording. As previously shown (Wakabayashi
420 et al., 2011), both PP and NP cells changed the sign of phototaxis when treated with
421 ROS-modulating agents. Our results demonstrate that the sign of phototaxis is
422 determined by which of the two (*cis*- and *trans*-) cilia beats stronger after
423 photoreception, and that the sign reverses depending on whether the dominant cilium
424 begins to beat stronger when the eyespot faces the light source or away from it (Fig. 8).
425 An important factor that modulates when the onset of ciliary dominance occurs is the
426 intracellular amount of ROS. Our mathematical model supports these findings.

427

428 **The cilium that becomes dominant after photoreception**

429 The first key factor that determines the phototactic sign is whether the *cis*- or the *trans*-
430 cilium is dominant in a given strain. Several previous studies have shown that the two
431 cilia of *C. reinhardtii* are intrinsically different (Kamiya & Hasegawa, 1987; Kamiya &
432 Witman, 1984; Rüffer & Nultsch, 1987, 1991, 1998). Rüffer and Nultsch (1991, 1998)
433 carried out high-speed cinematographic observation on cells trapped with a suction
434 pipette. They found that, upon photo-stimulation, the *trans*-cilium tended to beat more

435 strongly (with a larger amplitude and at a higher frequency) than the other in positively
436 phototactic strains, whereas the *cis*-cilium beat more strongly than the other in
437 negatively phototactic strains (Rüffer & Nultsch, 1991, 1998). Our results, obtained
438 from observation of free-swimming cells undergoing phototactic turning, are basically
439 consistent with these studies.

440 How is the dominant cilium determined? The results of the present study, as
441 well as those of Rüffer and Nultsch (1991), indicate that the cilium that becomes
442 dominant after photostimulation is the *trans*-cilium in PP and the *cis*-cilium in NP cells.
443 One would be inclined to assume that the Ca^{2+} sensitivities of the *cis*- and *trans*-
444 axonemes (the inner structure of cilia) are reversed between PP and NP. However, in
445 detergent-extracted and motility-reactivated cell models, the Ca^{2+}-dependent motility of
446 the two axonemes attached to a single cell body was found not to differ between PP and
447 NP strains (Wakabayashi et al., 2011). Therefore, factors other than axonemes may
448 cause differences in ciliary Ca^{2+}-response of PP and NP cells. For example, some
449 detergent-soluble constituents of cilia, or some chemical modification of the axoneme
450 that is not retained after detergent extraction, may be responsible.

451 Previously, we identified the defect that causes the negatively phototactic
452 phenotype in the NP strain (*agg1*) as the loss of a protein that possibly functions in

453 mitochondria (Ide et al., 2016). If this protein functions in the respiratory chain, the
454 redox poise and/or the amount of ROS could differ between PP and NP cells and
455 differentially modulate the activities of membrane proteins, such as Ca^{2+} channels and
456 pumps. Other *C. reinhardtii* mutants, *agg2* and *agg3*, are also known to display
457 negative phototaxis. Although whether the *cis*- or the *trans*-cilium is dominant in these
458 mutants has not been determined, their defects are also caused by mutations in non-
459 axonemal proteins; the causative protein Agg2 is localized to the proximal ciliary
460 membrane, while Agg3 is a flavodoxin that localizes to the ciliary matrix (Iomini, Li,
461 Mo, Dutcher, & Piperno, 2006). Loss of these proteins may modulate the function of the
462 ciliary membrane and could switch the dominant cilium.
463
464 **How is the off-response of the ciliary dominance produced?**
465 The second key factor that determines the phototactic sign is the timing at which the
466 dominant cilium starts to increase power after photoreception. We showed that *t*-
467 BOOH, a membrane-permeable ROS that promotes positive phototaxis, induces the
468 onset of *cis*-cilium dominance on the dark side in NP cells, whereas DMTU, a
469 membrane-permeable ROS-scavenger that promotes negative phototaxis, induces that of
470 the *trans*-cilium dominance on the dark side in PP cells (Fig. 2A, B). The onset of

471 ciliary dominance on the dark side could be interpreted as a so-called off response or a
472 step-down response, which means that cells respond to a light-off stimulus.

473 Off-response of *C. reinhardtii* has been suggested by Rüffer and Nultsch
474 (1991), but their "off-response" is different from what we observed for the majority of
475 cells showing the sign reversal. They showed that the beating in the two cilia
476 reciprocally changes upon reception of light-on as well as light-off stimuli: i.e., a strain
477 with the *trans* cilium that beats strongly for an on-response will have the *cis* cilium that
478 beats strongly for an off-response. Actually, their result is consistent with a minority of
479 our results. For example, when PP cells showed positive phototaxis, ~30% of the cells
480 beat their cis-cilium strongly when the eyespot faced the dark side (Fig. 2B). How the
481 majority and minority cells switch between the on- and off-responses that Rüffer and
482 Nultsch found was not clear from our experiments.

483 Off-response itself can be seen in other organisms; for example, in animal's
484 retina, the cells that normally excite upon light-on response excite upon light-off
485 response when the cells respond to glutamate, a neurotransmitter (Feher, 2012).
486 However, the molecular mechanism of the off response in *C. reinhardtii* is unknown.
487 Theoretically, a response equivalent to an off-response could be accomplished by an
488 appropriate delay in the light-on response. However, our observations on slow-

489 swimming mutants and PP cells in a viscous medium, as well as theoretical
490 considerations, rule out this possibility. Generally, the photoreception by ChR, a light-
491 gated cation channel, is thought to induce depolarization of the cellular membrane.
492 However, the Ca^{2+} influx at the eyespot may induce activation of Ca^{2+}-activated K^+
493 channel (Vergara et al., 1998), which would induce an increase in K^+ conductance and
494 concomitant hyperpolarization of the membrane. If the light causes hyperpolarization, a
495 light-off stimulus may induce depolarization of the membrane and elicit an off-
496 response. In addition, recently, ROS-modulating reagents were shown to modulate the
497 phosphorylation state of ChR1 (Bohm et al., 2019). The activity change of ChR1
498 according to this phosphorylation state may also lead to the off-response. These
499 possibilities can be tested by further electrophysiological analyses using ROS-
500 modulating reagents.
501
502 **Mathematical model results support the experimental data**
503 To mathematically assess the plausibility of the Dominant arm model and the Off-
504 response model, we developed a simple model that describes the swimming behaviors
505 of *C. reinhardtii*. The theoretical model and the experimental data both showed that the
506 Off-response model is not accomplished by the presence of a fixed delay time in the

507 light-on response, but by the response to a light-off stimulus (Figs. 5-7). While several
508 previous models have been presented to explain the photobehavior of green alga, ours is
509 one of the simplest, explaining the switching of the phototactic sign through only one
510 equation with some changes of the system parameters (Bennett & Golestanian, 2015;
511 Drescher et al., 2010).

512 Our model also provides clues to understanding why all the cells of the same
513 strain under the same light conditions do not exhibit the same sign of phototaxis; for
514 example, even when PP cells are treated with H_2O_2, which elicits positive phototaxis,
515 ~5% of the cells show negative phototaxis (Wakabayashi et al., 2011). This could be
516 explained by the variance of the delay time in the onset of ciliary dominance. Even
517 though our model precludes the fixed delay time after treatment with the ROS-
518 modulating reagents, the delay time may vary between cells. In Fig. 5, when $\gamma_0 = 1$
519 (i.e., the *trans*-cilium is dominant after photoreception) and $I_0 = 0.1$ or 0.5, cells show
520 positive phototaxis when ~50 < τ_0 < ~300 msec. The value of τ_0 has been suggested to
521 be longer than 30~40 msec (Rüffer & Nultsch, 1991; Witman, 1993). Thus, if a cell has
522 longer τ_0 than 300 msec, which would be caused by several factors including kinetics of
523 Ca^{2+} influx and cellular ROS amounts, this cell will exhibit negative phototaxis.
524 Furthermore, the τ_0-vz curves in Fig. 4 will change greatly if the eyespot position

525 somewhat varies and causes a change in the τ_0-vz curve. If a cell has the eyespot at an
526 irregular position, it may exhibit an opposite sign of phototaxis even with the same τ_0.
527 We must admit that our mathematical model has some drawbacks: it is based
528 on the major results of the observation. As mentioned earlier, there are exceptional
529 results; for example, ~30% of PP cells showed positive phototaxis with the dominant
530 beating of the *cis* cilium when the eyespot faces the dark side (Fig. 2B). It is still a
531 mystery as to whether cells choose the on- or off- response when exhibiting the same
532 sign of phototaxis. In this study, we took advantage of the fact that ROS-reagents can
533 bias the sign of phototaxis in either direction (Wakabayashi et al., 2011). Similarly, if
534 we can find conditions that bias either the on- or off-reaction, we may be able to derive
535 a model that encompasses all conditions.
536 In summary, our experimental observations combined with the insights from
537 our theoretical model showed that phototactic signs of *C. reinhardtii* cells are
538 determined by two factors: the genetically determined dominant cilium, and the timing
539 of the onset of strong beating by the dominant cilium after photoreception (Fig. 8). The
540 timing, either on the light side or the dark side, is modulated by the cellular amount of
541 ROS, which is a byproduct of photosynthesis. Cells may monitor photosynthetic
542 activities through ROS amounts, and this regulation mechanism may contribute to

543 maintaining ideal photosynthetic activities by modifying light conditions through

544 phototaxis.

545

546 **MATERIALS AND METHODS**

547 ***Cell culture and strains***

548 *Chlamydomonas reinhardtii* strains CC-124 (nit1− (nitrate reductase), nit2−, agg1−,

549 mt− (mating type)) (Ide et al., 2016), CC-125 (nit1−, nit2−, mt+), CC-2670 (ida4-,

550 mt+), and CC-2228 (oda1-, mt+) were used. CC-124 and CC-125 were termed PP and

551 NP, respectively. The CC-125 strain maintained in our laboratory appears to have a

552 slight difference in motility characteristics from the same strain available from the

553 Chlamydomonas Resource Center (http://www.chlamycollection.org/) (Sato, Sato, &

554 Toyoshima, 2018; Wakabayashi et al., 2011). CC-2670 (*ida4*; lacking inner-arm

555 dyneins a, c, and d) and CC-2228 (*oda1*; lacking outer-arm dynein and the outer-dynein

556 arm docking complex) were used as slow-swimming mutants. Cells were grown in tris-

557 acetate phosphate medium (TAP) medium with aeration at 25 °C, on a 12 h/12 h

558 light/dark cycle (Gorman & Levine, 1965).

559

560 ***High-speed observation of phototaxis and measurement of the bodily rotation cycle***

561 Cells were washed with an experimental solution (5 mM Hepes (pH 7.4), 0.2 mM

562 EGTA, 1 mM KCl, 0.3 mM $CaCl_2$) (Okita, Isogai, Hirono, Kamiya, & Yoshimura,

563 2005) and kept under red light for more than 50 minutes before the assays. To induce

564 positive or negative phototaxis, the cell suspensions were treated with tertiary-
565 butylhydroperoxide (*t*-BOOH; final concentration is 0.2 mM) (Wako Pure Chemical
566 Industries) as a ROS reagent, or dimethylthiourea (DMTU; final concentration is 75
567 mM) (Sigma-Aldrich) as a ROS-scavenging reagent (Wakabayashi et al., 2011). Cell
568 suspensions were put between a coverslip and a glass slide and placed on the stage of a
569 dark-field microscope with an oil-immersion condenser (BX53; Olympus). The
570 directional light to induce phototaxis was produced with two green LEDs (λ=525 nm).
571 The setup is shown in Fig. 2A. First, a weak green light (~5 μmol photons m^{-2} s^{-1}) was
572 illuminated (Light 1 in Fig. 2A). Most cells showed either positive or negative
573 phototaxis. Then a stronger green light (Light 2 in Fig. 2A; ~30 μmol photons m^{-2} s^{-1})
574 was illuminated, perpendicular to Light 1. Most of the cells then changed their
575 swimming directions and oriented parallel to the Light 2 beam. The behavior of cells
576 was observed with dim red light (λ >600 nm) and videos were recorded with a high-
577 speed camera (HAS-L2M, DITECT) at 150 fps. The LED for Light 2 was linked with
578 the trigger switch of the high-speed camera so that recording was initiated when it was
579 lit. The timing of photoreception was determined as the time when the eyespot faced the
580 Light 2 side (Fig. 2A, 2B). The position of the eyespot in the helical swimming paths
581 was also determined from the same video footage.

582 The measurement of the bodily rotation cycle was carried out with the same
583 experimental setup as above (without sideways illuminations). The time required for
584 one bodily rotation was determined from the position of the eyespot on the swimming
585 trajectories, and the rotation period was calculated.
586
587 ***Phototaxis assay***
588 The phototaxis assay shown in Fig. 5 was carried out by the method described in (Ueki
589 et al., 2016). In brief, cells were washed with the experimental solution and kept under
590 dim red light for 30 min before the phototaxis assays. For dish assays, cell suspensions
591 (~10^7 cells/mL) were put in Petri dishes (30 mm in diameter, 10 mm thick), illuminated
592 with a green LED (λ =525 nm, ~50 μmol photons m^{-2} s^{-1}) from one side for 5 min, and
593 photographed (DSC-RX100M2; Sony). For preparation of viscous media, 4.5% or 9.0%
594 Ficoll (Mw 400; 16006-92, Nacalai) was added to the experimental solution. For single-
595 cell analysis, cells were observed under a dark-field microscope (BX-53, Olympus)
596 under dim red light (λ > 600 nm) and recorded to video using a CCD camera
597 (1129HMN1/3; Wraymer). The angle (θ) between the light direction and the swimming
598 direction was measured for 1.5 s, following illumination with a green LED for 15 s.
599 Images of swimming cells were auto-tracked using Image Hyper software (Science

600 Eye), and angles were measured from the cell trajectories. *t*-BOOH (final concentration

601 of 0.2 mM; Wako Pure Chemical Industries) was used as a ROS reagent, and

602 dimethylthiourea (final concentration of 75 mM; Sigma-Aldrich) was used as a ROS-

603 scavenging reagent

604

605 ***Electrophysiology***

606 PRCs were assessed in a population of *C. reinhardtii* cells by the method

607 of Sineshchekov et al. (1992) (O. A. Sineshchekov et al., 1992, 1994). In brief, 1 ml of

608 cell suspension in a measuring solution (0.5 mM Hepes, pH 7.3, 0.1 mM $CaCl_2$) was put

609 in a cuvette (10×10×15 mm), with two electrodes on each side of its rectangular bottom.

610 A 500 nm beam of light was generated with an LED source (NSPE510S, Nichia

611 Chemical) and applied from one side of the electrode. The current was measured with a

612 patch-clamp amplifier (Axoclamp 200B, Axon).

613

614 ***Measurement of ciliary beating frequency***

615 Ciliary beating frequency (CBF) was measured based on the method described in (R

616 Kamiya, 2000) with modifications (Wakabayashi & King, 2006). The median frequency

617 was obtained from the power spectra of fast Fourier-transformed cell body vibration

618 signals in microscopy images averaged for ~20 s.

619

620 ***Measurement of bodily rotation cycle***

621 Cells were observed under a dark-field microscope with an oil-immersion condenser

622 (BX-53, Olympus) and recorded to video with a high-speed camera (HAS-L2M,

623 DITECT) at 150 fps. The bodily rotation cycle was defined as the time it takes for the

624 eyespot (observed as a bright spot) to return to the same position relative to the cell's

625 swimming trajectory, and was measured by counting the frames for one cycle.

626

627

628

Acknowledgments

This work was supported by Japan Society for the Promotion of Science KAKENHI Grants 19H03242, 20K21420, 21H00420, 22H02642, and 22H05674 to KW, 16H06556 to TH, 17H02939 to KS, 17K07370 to KY, 19K23758 to NU, by Ohsumi Frontier Science Foundation to KW, by Global Station for Soft Matter at Hokkaido University to KS and TN, by Dynamic Alliance for Open Innovation Bridging Human, Environment and Materials to TH, KS, TN, and KW and by the Japan Agency for Medical Research and Development (AMED/PRIME) grant JP18gm5810013 to KY.

Competing interests

The authors declare that no competing interests exist.

References

Bennett, R. R., & Golestanian, R. (2015). A steering mechanism for phototaxis in Chlamydomonas. *J R Soc Interface, 12*(104), 20141164.

Bohm, M., Boness, D., Fantisch, E., Erhard, H., Frauenholz, J., Kowalzyk, Z., . . . Kreimer, G. (2019). Channelrhodopsin-1 Phosphorylation Changes with Phototactic Behavior and Responds to Physiological Stimuli in Chlamydomonas. *Plant Cell, 31*(4), 886-910.

Drescher, K., Goldstein, R. E., & Tuval, I. (2010). Fidelity of adaptive phototaxis. *Proc Natl Acad Sci U S A, 107*(25), 11171-11176.

Feher, J. (2012). In *Quantitative Human Physiology*, Elsevier Inc.

Feinleib, M. E. H., & Curry, G. M. (1971). The relationship between stimulus intensity and oriented phototactic response (topotaxis) in Chlamydomonas. In *Physiologia Plantarum* (Vol. 25, pp. 346-352).

Foster, K. W., & Smyth, R. D. (1980). Light Antennas in phototactic algae. *Microbiol Rev, 44*(4), 572-630.

Gorman, D. S., & Levine, R. P. (1965). Cytochrome f and plastocyanin: their sequence in the photosynthetic electron transport chain of Chlamydomonas reinhardi. *Proc Natl Acad Sci U S A, 54*(6), 1665-1669.

Ide, T., Mochiji, S., Ueki, N., Yamaguchi, K., Shigenobu, S., Hirono, M., & Wakabayashi, K.-i. (2016). Identification of the agg1 mutation responsible for negative phototaxis in a “wild-type” strain of Chlamydomonas reinhardtii. *Biochemistry and Biophysics Reports, 7*, 379-385.

Iomini, C., Li, L., Mo, W., Dutcher, S. K., & Piperno, G. (2006). Two flagellar genes, AGG2 and AGG3, mediate orientation to light in Chlamydomonas. *Curr Biol, 16*(11), 1147-1153.

Isogai, N., Kamiya, R., & Yoshimura, K. (2000). Dominance between the two flagella during phototactic turning in Chlamydomonas. *Zool Sci, 17*, 1261-1266.

Kamiya, R. (1988). Mutations at twelve independent loci result in absence of outer dynein arms in Chlamydomonas reinhardtii. *J Cell Biol, 107*(6 Pt 1), 2253-2258.

Kamiya, R. (2000). Analysis of cell vibration for assessing axonemal motility in Chlamydomonas. *Methods, 22*, 383-387.

Kamiya, R., & Hasegawa, E. (1987). Intrinsic difference in beat frequency between the two flagella of Chlamydomonas reinhardtii. *Exptl. Cell Res., 173, 299-304*.

Kamiya, R., Kurimoto, E., & Muto, E. (1991). Two types of Chlamydomonas flagellar mutants missing different components of inner-arm dynein. *J Cell Biol, 112*(3),

441-447.
Kamiya, R., & Witman, G. B. (1984). Submicromolar levels of calcium control the balance of beating between the two flagella in demembranated models of Chlamydomonas. *J Cell Biol, 98*(1), 97-107.
Kondo, T., Johnson, C. H., & Hastings, J. W. (1991). Action spectrum for resetting the circadian phototaxis rhythm in the CW15 strain of Chlamydomonas 1. Cells in darkness. *Plant Physiol, 95,* 197-205.
Landau, L. D., Lifshitz, E. M. (1976). *Mechanics, 3rd ed.* (Vol. 1 (Course of Theoretical Physics)): Oxford: Butterworth- Heinemann.
Leptpos, K. C., Chioccioli, M., Furlan, S., Pesci, A. I., & Goldstein, R.E. (2018) An Adaptive Flagellar Photoresponse Determines the Dynamics of Accurate Phototactic Steering in *Chlamydomonas. bioRxiv,* doi: 10.1101/254714 version 2.
Morel-Laurens, N. (1987). Calcium control of phototactic orientation in Chlamydomonas reinhardtii: sign and strength of response. *Photochem Photobiol, 45*(1), 119-128.
Nagel, G., Ollig, D., Fuhrmann, M., Kateriya, S., Musti, A. M., Bamberg, E., & Hegemann, P. (2002). Channelrhodopsin-1: a light-gated proton channel in green algae. *Science, 296*(5577), 2395-2398.
Nagel, G., Szellas, T., Huhn, W., Kateriya, S., Adeishvili, N., Berthold, P., . . . Bamberg, E. (2003). Channelrhodopsin-2, a directly light-gated cation-selective membrane channel. *Proc Natl Acad Sci U S A, 100*(24), 13940-13945.
Okita, N., Isogai, N., Hirono, M., Kamiya, R., & Yoshimura, K. (2005). Phototactic activity in Chlamydomonas 'non-phototactic' mutants deficient in Ca2+-dependent control of flagellar dominance or in inner-arm dynein. *J Cell Sci, 118*(3), 529-537.
Rüffer, U., & Nultsch, W. (1987). Comparison of the beating of cis- and trans-flagella of Chlamydomonas cells held on micropipettes. *Cell Motil Cytoskeleton, 7*, 87-93.
Rüffer, U., & Nultsch, W. (1998). Flagellar coordination in Chlamydomonas cells held on micropipettes. *Cell Motil Cytoskeleton, 41*(4), 297-307.
Rüffer, U., & Nultsch, W. (1991). Flagellar photoresponses of Chlamydomonas cells held on micropipettes: II. Change in flagellar beat pattern. *Cell Motility Cytoskeleton, 18*(4), 269-278.
Sato, N., Sato, K., & Toyoshima, M. (2018). Analysis and modeling of the inverted bioconvection in Chlamydomonas reinhardtii: emergence of plumes from the layer of accumulated cells. *Heliyon, 4*(3), e00586.
Sineshchekov, O. A., Govorunova, E. G., Der, A., Keszthelyi, L., & Nultsch, W. (1992). Photoelectric Responses in Phototactic Flagellated Algae Measured in Cell-

Suspension. *J Photochem Photobiol B-Biology, 13*(2), 119-134.

Sineshchekov, O. A., Govorunova, E. G., Der, A., Keszthelyi, L., & Nultsch, W. (1994). Photoinduced electric currents in carotenoid-deficient Chlamydomonas mutants reconstituted with retinal and its analogs. *Biophys J, 66*(6), 2073-2084.

Sineshchekov, O. A., Jung, K.-H., & Spudich, J. L. (2002). Two rhodopsins mediate phototaxis to low- and high-intensity light in Chlamydomonasreinhardtii. *PNAS, 99*(13), 8689-8694.

Suzuki, T., Yamasaki, K., Fujita, S., Oda, K., Iseki, M., Yoshida, K., . . . Takahashi, T. (2003). Archaeal-type rhodopsins in Chlamydomonas: model structure and intracellular localization. *Biochem Biophys Res Commun, 301*(3), 711-717.

Takada, S., Wilkerson, C. G., Wakabayashi, K., Kamiya, R., & Witman, G. B. (2002). The outer Dynein arm-docking complex: composition and characterization of a subunit (oda1) necessary for outer arm assembly. *Mol Biol Cell, 13*(3), 1015-1029.

Takahashi, T., & Watanabe, M. (1993). Photosynthesis modulates the sign of phototaxis of wild-type Chlamydomonas reinhardtii. Effects of red background illumination and 3-(3',4'-dichlorophenyl)-1,1-dimethylurea. *FEBS Lett, 336*(3), 516-520.

Ueki, N., Ide, T., Mochiji, S., Kobayashi, Y., Tokutsu, R., Ohnishi, N., . . . Wakabayashi, K. (2016). Eyespot-dependent determination of the phototactic sign in Chlamydomonas reinhardtii. *Proc Natl Acad Sci U S A, 113*(19), 5299-5304.

Vergara, C., Latorre, R., Marrion, N. V., & Adelman, J. P. (1998). Calcium-activated potassium channels. *Curr Opin Neurobiol, 8*(3), 321-329.

Wakabayashi, K., & King, S. M. (2006). Modulation of Chlamydomonas reinhardtii flagellar motility by redox poise. *J Cell Biol, 173*(5), 743-754.

Wakabayashi, K., Misawa, Y., Mochiji, S., & Kamiya, R. (2011). Reduction-oxidation poise regulates the sign of phototaxis in Chlamydomonas reinhardtii. *Proc Natl Acad Sci U S A, 108*(27), 11280-11284.

Witman, G. B. (1993). Chlamydomonas phototaxis. *Trends Cell Biol, 3*, 403-408.

740 **Table 1. Ciliary beating frequencies and bodily rotation cycles of strains used**

	PP	NP	*ida4*	*oda1*
Ciliary Beating Frequency (Hz) (Mean ± SEM, n=3 measurements)	55.0 ± 0.6	55.5 ± 1.0	51.6 ± 2.6	24.3 ± 0.6
Bodily rotation cycle (Hz) (Mean ± SD, n=10 cells)	2.11 ± 0.27	1.89 ± 0.27	1.25 ± 0.22	0.72 ± 0.09

741 **Table 2. Swimming parameters of PP in a solution containing Ficoll400**

	PP in 4.5% Ficoll	PP in 9.0% Ficoll
Ciliary Beating Frequency (Hz) (Mean ± SEM, n=3 measurements)	38.2 ± 0.21	26.8 ± 1.35
Bodily rotation cycle (Hz) (Mean ± SD, n=10 cells)	2.13 ± 0.77	0.91 ± 0.24
Swimming velocity (μm/s) (Mean ± SD, n=20 cells)	105.9 ± 31.9	50.7 ± 12.6

742

743

744 **Figure legends**

745 **Fig. 1**

746 **Schematic images of a *Chlamydomonas reinhardtii* cell and its phototaxis.**

747 **(A)** Schematic image of *C. reinhardtii* cell and the eyespot. The cilium closest to the

748 eyespot is called *cis*-cilium, whereas the one farthest from the eyespot is called *trans*-

749 cilium. The eyespot is composed of the carotenoid-rich granule layers that function as a

750 light reflector, and channelrhodopsin molecules aligned in the plasma membrane.

751 Channelrhodopsin functions as a light-gated cation channel. The light signal coming

752 from the outside of the cell is reflected by the carotenoid granule layers and amplified,

753 whereas that coming through the cell is blocked. (B) The current model to explain

754 positive phototaxis. After photoreception at the eyespot (yellow arrow), $[Ca^{2+}]_i$ in the

755 cilia increases and the *trans*-cilium (t) becomes dominant. After a half rotation of the

756 cell around its central axis, the light signal to the eyespot is blocked, $[Ca^{2+}]_i$ in the cilia

757 decreases, and the *cis*-cilium (c) becomes dominant. (C) Hypothetical models for

758 negative phototaxis. In the "Dominant arm model", Ca^{2+}-sensitivities of two cilia are

759 assumed to be reversed from the positively phototactic cell shown in (B); the *cis*-cilium

760 becomes dominant after photoreception. In the "Off-response model", after

761 photoreception, the *trans*-cilium becomes dominant when the eyespot faces opposite to

762 the light source.

763

764 **Fig. 2**

765 **Eyespot position relative to the cell trajectory during phototaxis.**

766 **(A)** Phototactic turnings of PP and NP cells after treatment with t-BOOH or DMTU.

767 Images of a swimming cell, taken at 150 fps, are superimposed every 0.13 sec. First,

768 Light 1 (weak green light from the left) was illuminated to induce positive (top;

769 swimming to the left) or negative (bottom; swimming to the right) phototaxis. After

770 Light 2 (strong green light from the top) was turned on, the cell changed its swimming

771 direction. The timing of the onset of Light 2 was at the white arrows/arrowhead. The

772 eyespot facing Light 2 is shown with green arrowheads, whereas that facing opposite to

773 Light 2 is shown with magenta arrowheads. The former case is classified as "the light

774 side") and the latter "the dark side" in **(B).** Yellow arrows show the swimming

775 directions. (The cells whose trajectories intersect with the superimposed cells were

776 removed from the image in the process creating the superimpose. See SI Movies S1-4

777 for the raw data.) **(B)** The proportion of the dominant cilium and the side where the

778 onset of the ciliary dominance occurred. PP cells showing positive phototaxis (control

779 and +*t*-BOOH) or negative phototaxis (+DMTU) and NP cells showing negative

780 phototaxis (control and +DMTU) or positive phototaxis (+*t*-BOOH) were observed

781 (n=8~28 per condition).

782

783 **Fig. 3**

784 **Mathematical model for *C. reinhardtii* phototaxis.**

785 **(A)** Definitions of the body axes of a *C. reinhardtii* cell. The vectors **a**, **b** and **c** are unit

786 vectors that are fixed to the body of the cell. **a**, **b** and **c** are mutually orthogonal to each

787 other, and **b** and **c** are within the ciliary beat plane. **b** is close to the side of *cis*-cilium.

788 With them, the direction of eyespot is expressed as $\mathbf{e}_{eyespot} = (\mathbf{b}+\mathbf{c})/\sqrt{2}$. The directions

789 of **a**, **b** and **c** evolve with time according to Eq. 1. **(B)** Definitions of the Euler angles

790 that specify the directions of **a**, **b**, **c** for the x, y, z coordinate system that is fixed in

791 space. θ_1 is the angle between the y-axis and the vector $\mathbf{N}$, where $\mathbf{N} = \mathbf{z}\times\mathbf{c}/|\mathbf{z}\times\mathbf{c}|$.

792 θ_2 and θ_3 are angles between the z-axis and $\mathbf{c}$ and between $\mathbf{N}$ and $\mathbf{b}$,

793 respectively. When $\theta_1 = \theta_2 = \theta_3 = 0$, **a**, **b**, **c** axes coincide with x, y, z axes,

794 respectively. **(C), (D)** Examples of initial trajectories of the cell obeying Eq. 1

795 ($0 \le t \le 10$), which indicate positive phototaxis (τ_0=0.08 sec, **(C)**) and negative

796 phototaxis (τ_0=0.32 sec. **(D)**). The parameters are $\gamma_0 = 1$ (the *trans*-cilium becomes

dominant after photoreception at the eyespot), $I_0 = 0.5$, $v_0 = 128$ [μm/s], [1/s], $\omega_c = -11.8$ [1/s] and $\omega_a = 5.8$ [1/s]. The initial conditions are $\mathbf{r}(0) = (0,0,0)$, $\theta_1(0) = 0$, $\theta_2(0) = -\pi/2$ and $\theta_3(0) = 0$. Thick orange arrows show the direction of the light illumination, and thin black arrows show the swimming direction of the cell.

Fig. 4

Sign-switching of phototaxis in the mathematical model.

The mean velocity $\bar{v}_z$ of the steady-state of the cell after a long-time simulation as a function of the delay time τ_0 for various values of γ_0 and I_0. For each set of system parameters, only one steady state of Eq. 1 realizes, which does not depend on the initial conditions of θ_1, θ_2, θ_3, $\mathbf{r}$. $\bar{v}_z$ changes with τ_0; especially, the sign of $\bar{v}_z$ (=the sign of phototaxis) changes with γ_0 and τ_0. Blue dots are the states where solution S5 realizes, while red dots are the states where solution S6 realizes. Black dots with bars are the states where solutions other than Eqs. S5 or S6 are achieved, in which $v_z(t)$ oscillates in time. The bars indicate the standard deviation of v_z of the steady-state. The parameter values used are $v_0 = 128$ [μm/s], [1/s], $\omega_c = -11.8$ [1/s] and $\omega_a = 5.8$ [1/s]. The initial conditions are: $\mathbf{r}(0) = (0,0,0)$, $\theta_i(0) = \delta_i$ with random numbers $\delta_i \in [0, 2\pi]$ for $i = 1,2,3$, and $dI(t)/dt = 0$ for $0 \le t \le \tau_0$. For the discretization of

815 Eq. S1, the Euler method was used ($\Delta t = 1/10000$). The model suggests that, when γ_0

816 =1 (i.e. the *trans*-cilium is dominant), the cell shows positive phototaxis (i.e. γ_0 is

817 positive) when the dominant cilium beats stronger than the *cis*-cilium with the delay

818 (τ_0) 60~280 ms. Similarly, when γ_0=-1 (i.e. the *cis*-cilium is dominant), the cell shows

819 negative phototaxis under the same conditions.

820

821 **Fig. 5**

822 **Phototaxis assay of the slow-swimming cells.**

823 **(A)** PP, NP, *oda1*, and *ida4* cell suspensions put in Petri dishes with or without ROS-

824 modulating reagents (0.2 mM *t*-BOOH or 75 mM DMTU) were illuminated by green

825 LED (λ=525 nm, 30 μmol photons m^{-2} s^{-1}) from the right (green arrows) for 5 min from

826 the right. Cells showing positive phototaxis are accumulated in the right halves of the

827 dishes (orange boxes with "P") and those showing negative phototaxis are accumulated

828 in the left halves of the dishes (blue boxes with "N"). **(B)** Polar histograms depicting the

829 percentage of cells moving in a particular direction relative to light illuminated from the

830 right (green arrows), with or without treatment with ROS-modulating reagents (12 bins

831 of 30°; n = 30 cells per condition).

832

833 **Fig. 6**

834 **Phototaxis assay of PP cells in viscous media.**

835 (A) PP cells in viscous media (containing 4.5% or 9.0% Ficoll400) after treatment with

836 75 mM DMTU were illuminated by green LED (λ=525 nm, 30 μmol photons m^{-2} s^{-1})

837 from the right (green arrows) for 5 min from the right. **(B)** Polar histograms depicting

838 the percentage of cells moving in a particular direction relative to light illuminated from

839 the right (green arrows) (12 bins of 30°; n = 30 cells per condition).

840

841

842

Fig. 7

Sign-switching of phototaxis in a slow-swimming mutant in the mathematical model.

The plots of the mean velocity $\bar{v}_z$ of the steady-state of the mathematical model (Eqs. S3 and S4 in SI Appendix A) as a function of the delay time τ_0 for two cells: (A) *ida4* (rotation frequency 1.25 Hz) and (B) *oda1* (rotation frequency 0.72 Hz), which rotation rates are much slower than that of PP cell (2 Hz). The parameter values used here are (A) $v_0 = 69$ [μm/s], $\omega_c = -6.3$ [1/s] and $\omega_a = 4.6$ [1/s], (B) $v_0 = 57$ [μm/s], $\omega_c = -4.0$ [1/s] and $\omega_a = 2.1$ [1/s], which are obtained from experimental data and Eq. (3). The meanings of blue, red, and black dots and bars in this figure are the same as those in Fig. 4.

Fig. 8

Schematic model of sign-reversal in phototaxis suggested by this study.

To make a phototactic turning, *cis*-dominant strain beats the *cis*-cilium (C) stronger than the *trans*-cilium (T), whereas *trans*-dominant strain beats the *trans*-cilium stronger than the *cis*-cilium. The *trans*-dominant strain, such as PP in this study, shows positive

861 phototaxis when the strong beating occurs upon light-on response (i.e. when the eyespot

862 faces the light side) and negative phototaxis when it occurs upon light-off response (i.e.

863 when the eyespot faces the dark side). The *cis*-dominant strain, such as NP in this study,

864 shows negative phototaxis when the strong beating occurs upon light-on response and

865 positive phototaxis when it occurs light-off response.

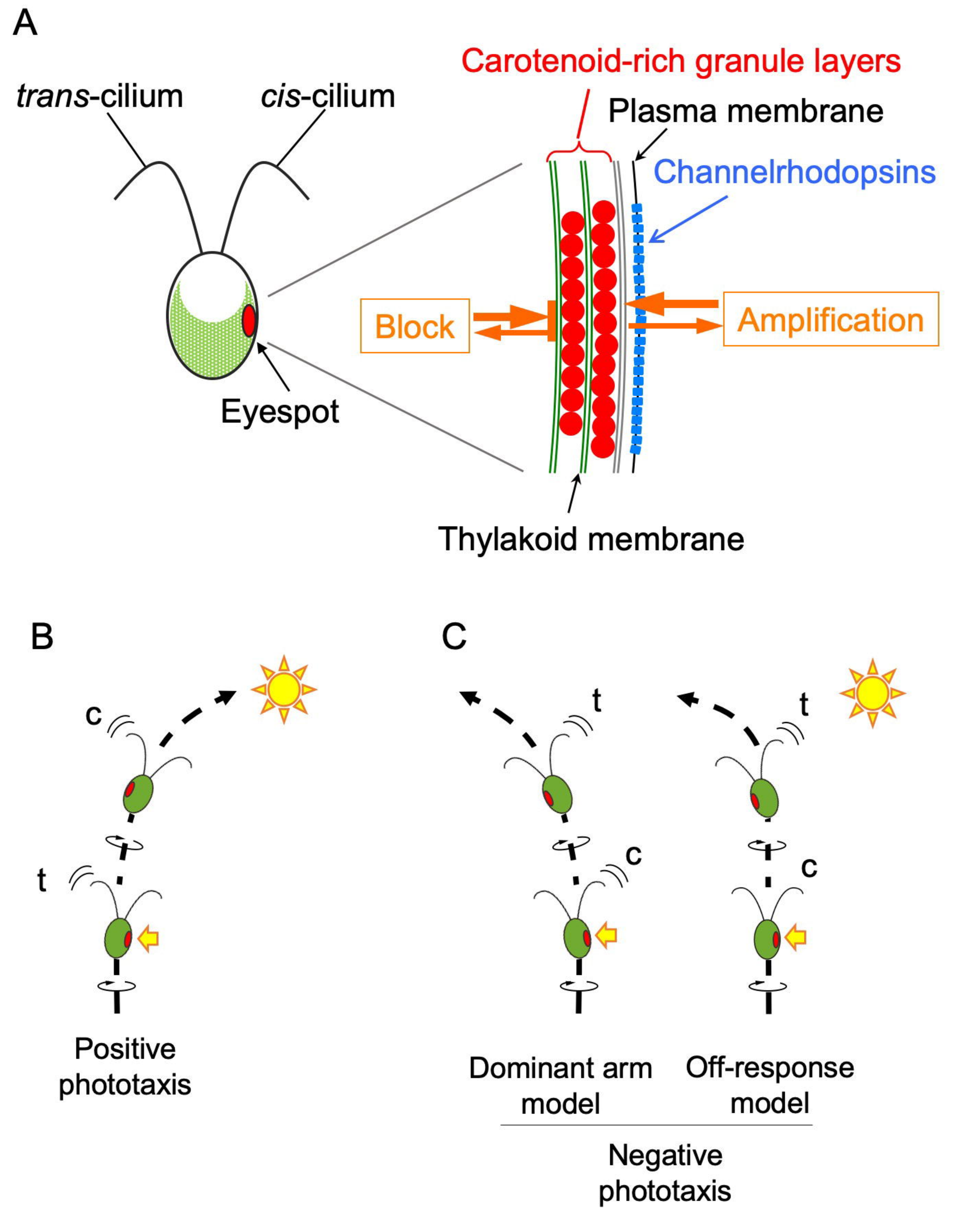

Fig. 1 **Schematic images of a *Chlamydomonas reinhardtii* cell and its phototaxis.**

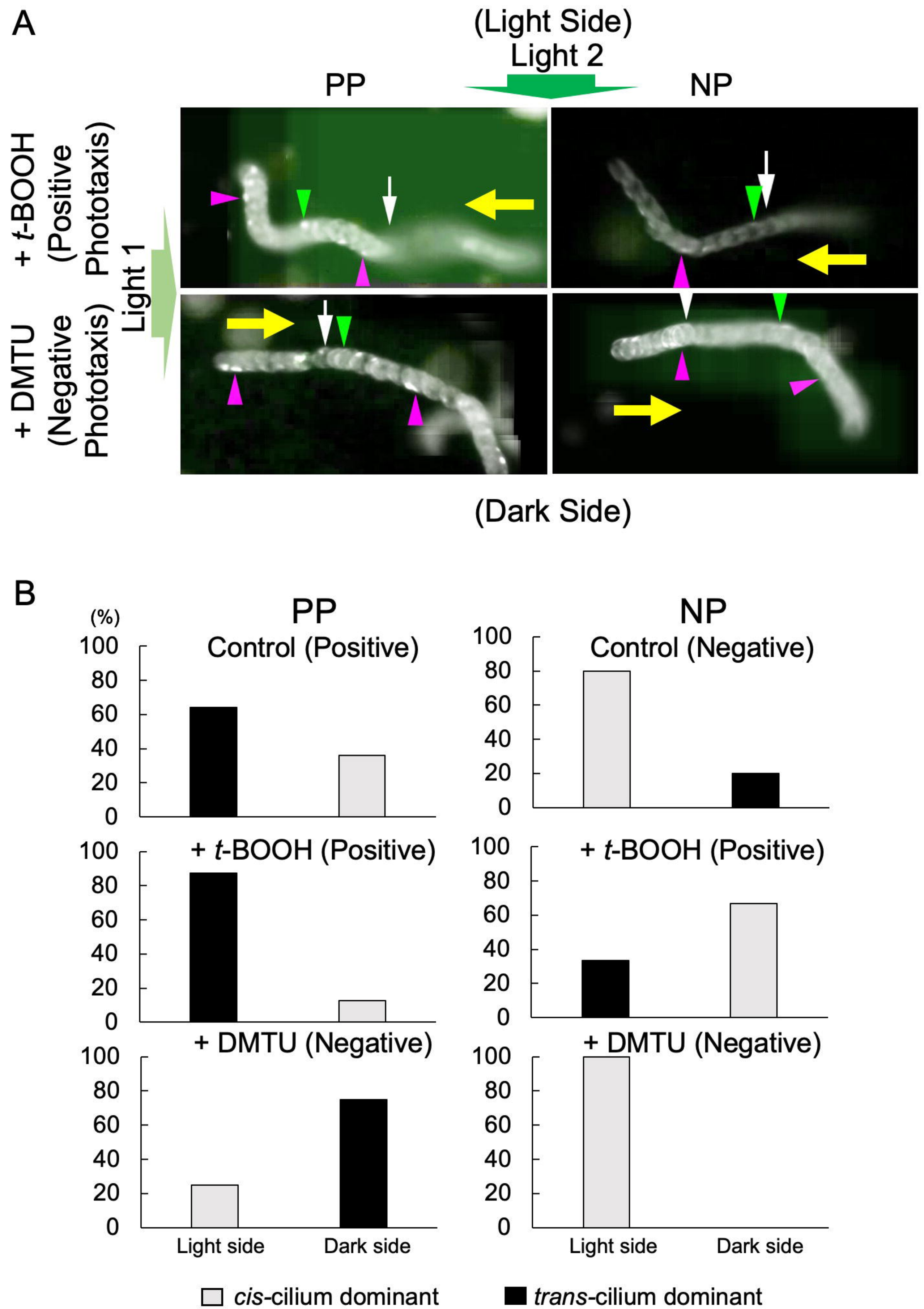

Fig. 2 **Eyespot position relative to the cell trajectory during phototaxis.**

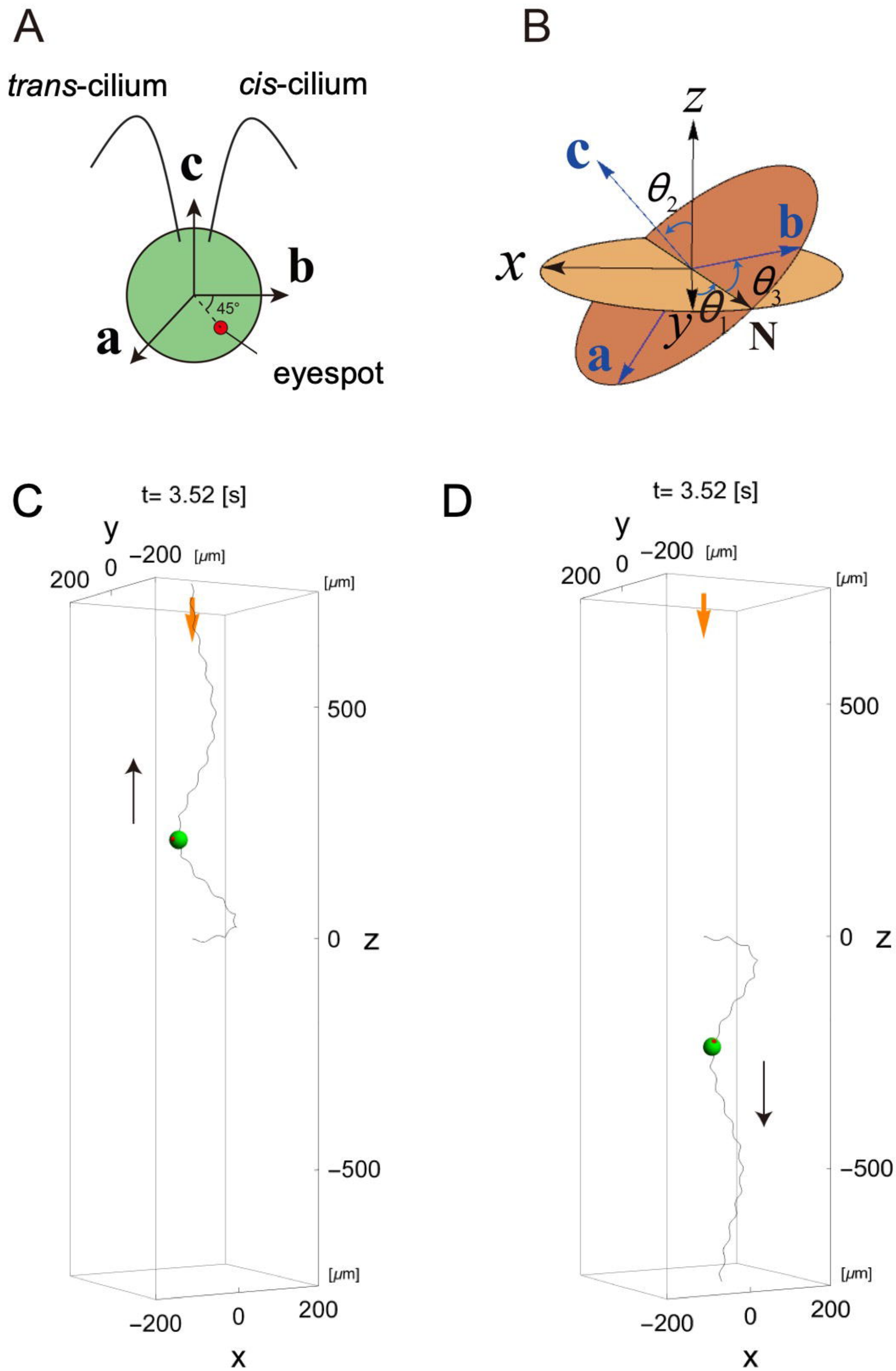

Fig. 3 **Mathematical model for *C. reinhardtii* phototaxis.**

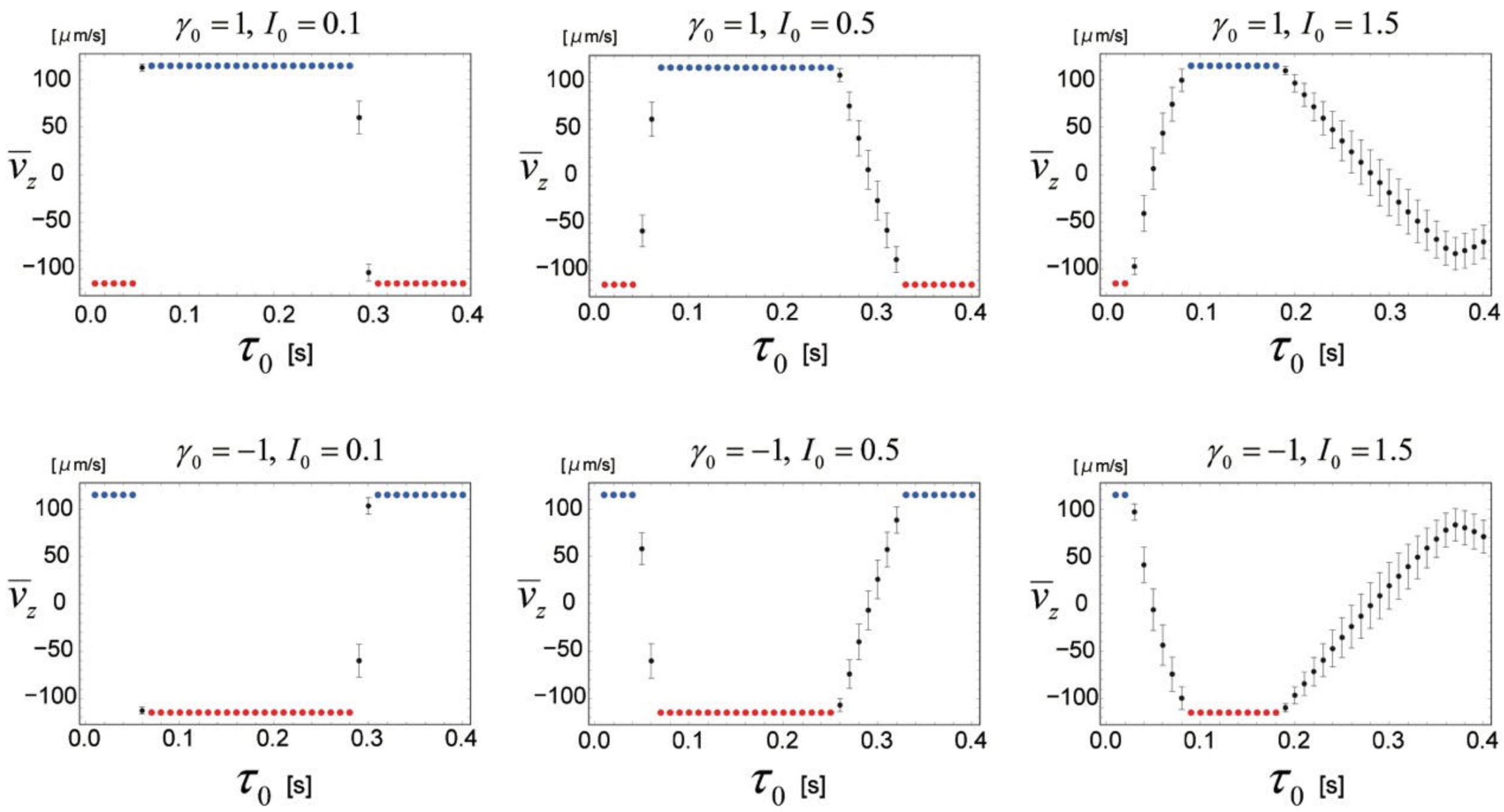

Fig. 4 **Sign-switching of phototaxis in the mathematical model.**

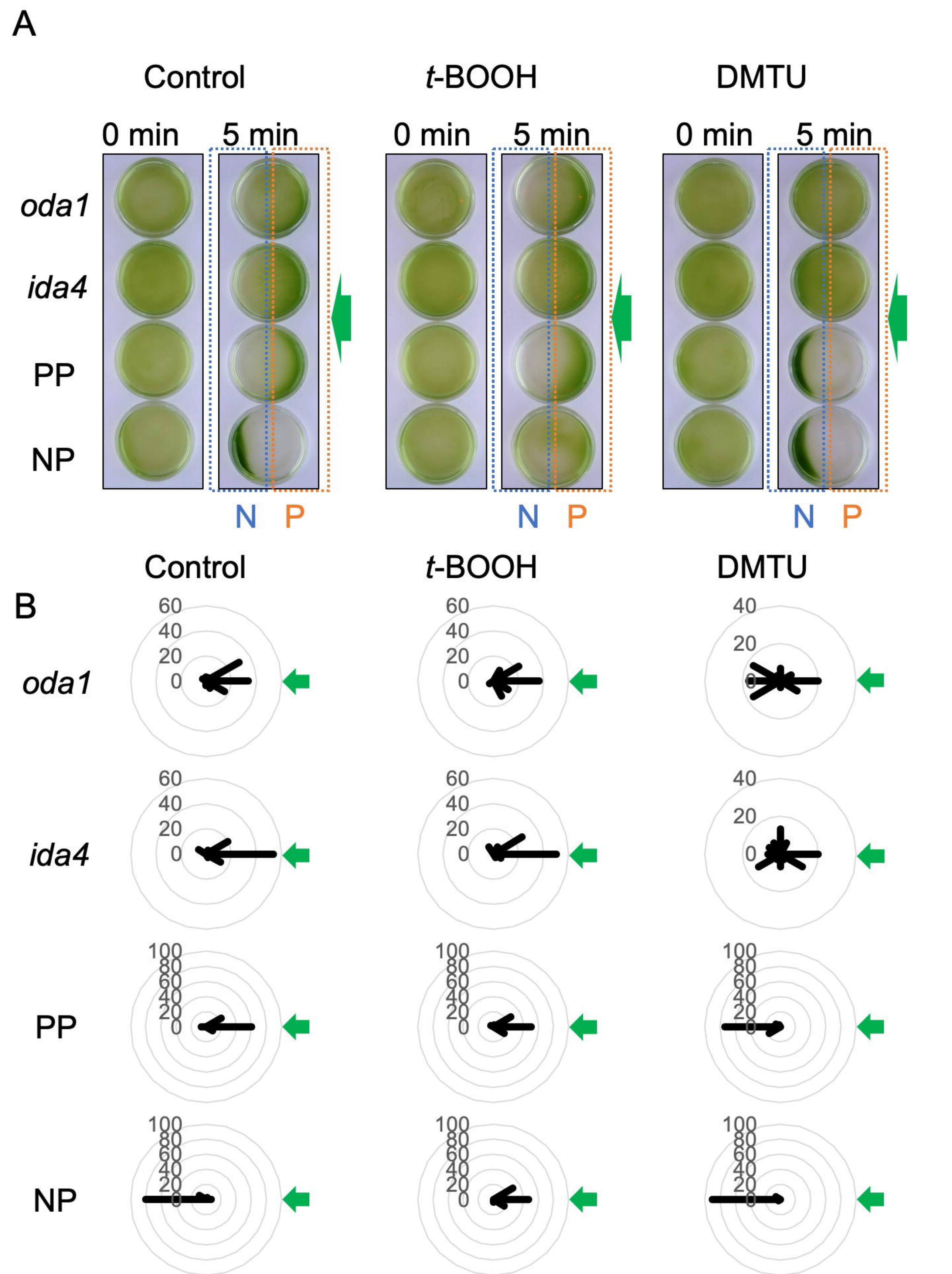

Fig. 5 **Phototaxis assay of the slow-swimming mutants.**

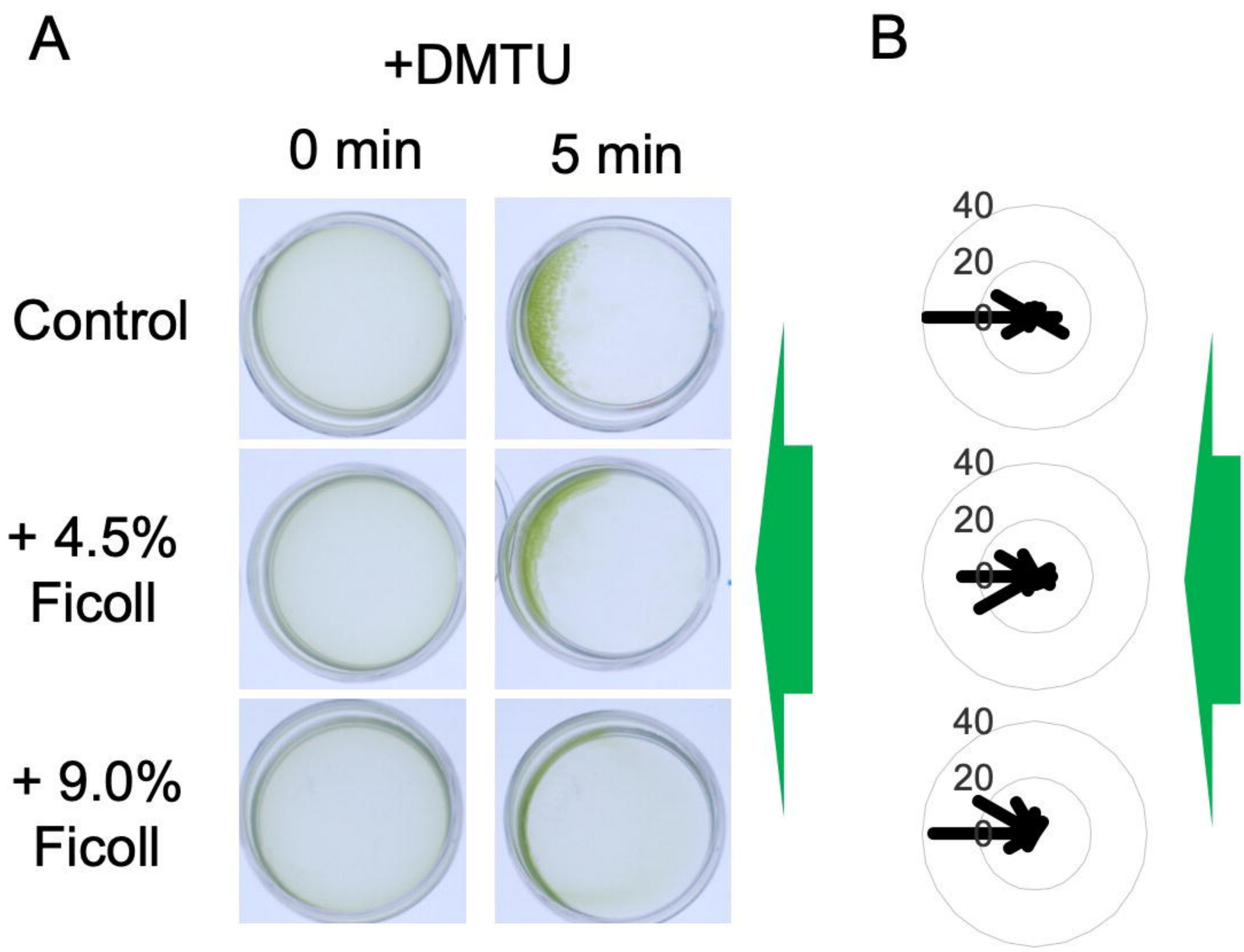

Fig. 6 **Phototaxis assay of PP in viscous media.**

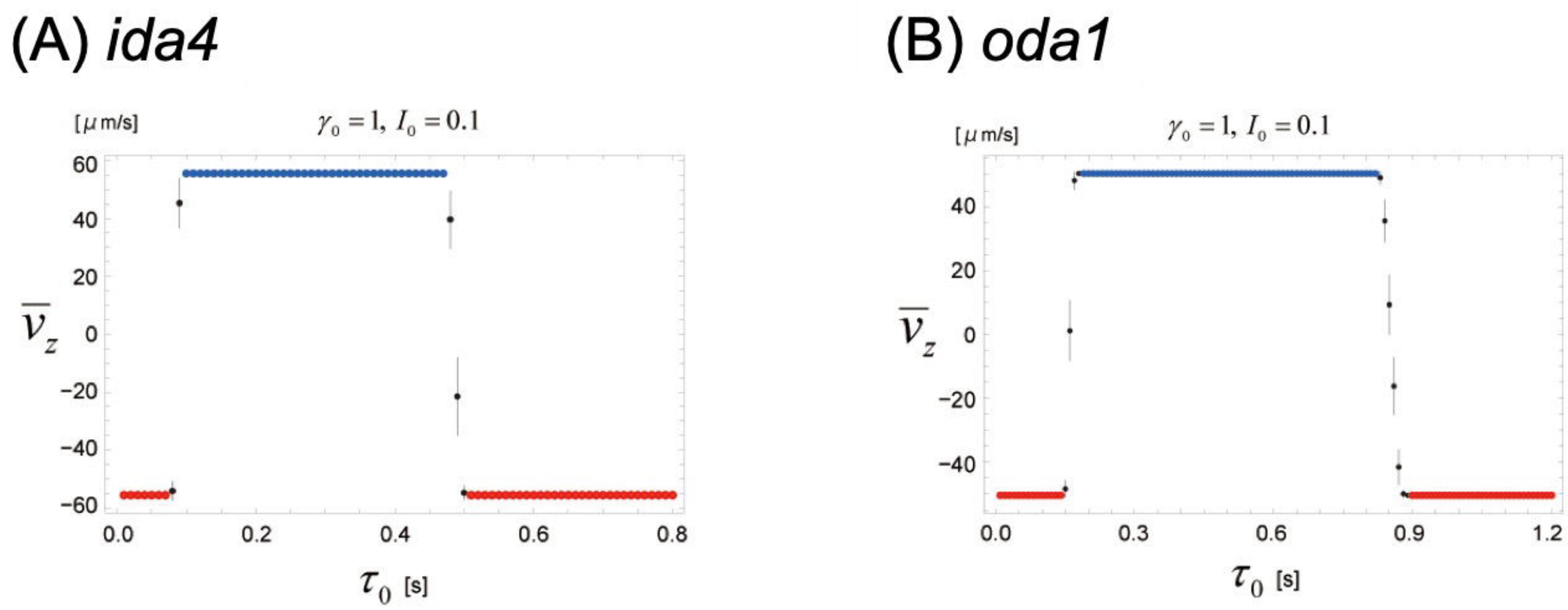

Fig. 7 **Sign-switching of phototaxis in a slow-swimming mutant in the mathematical model.**

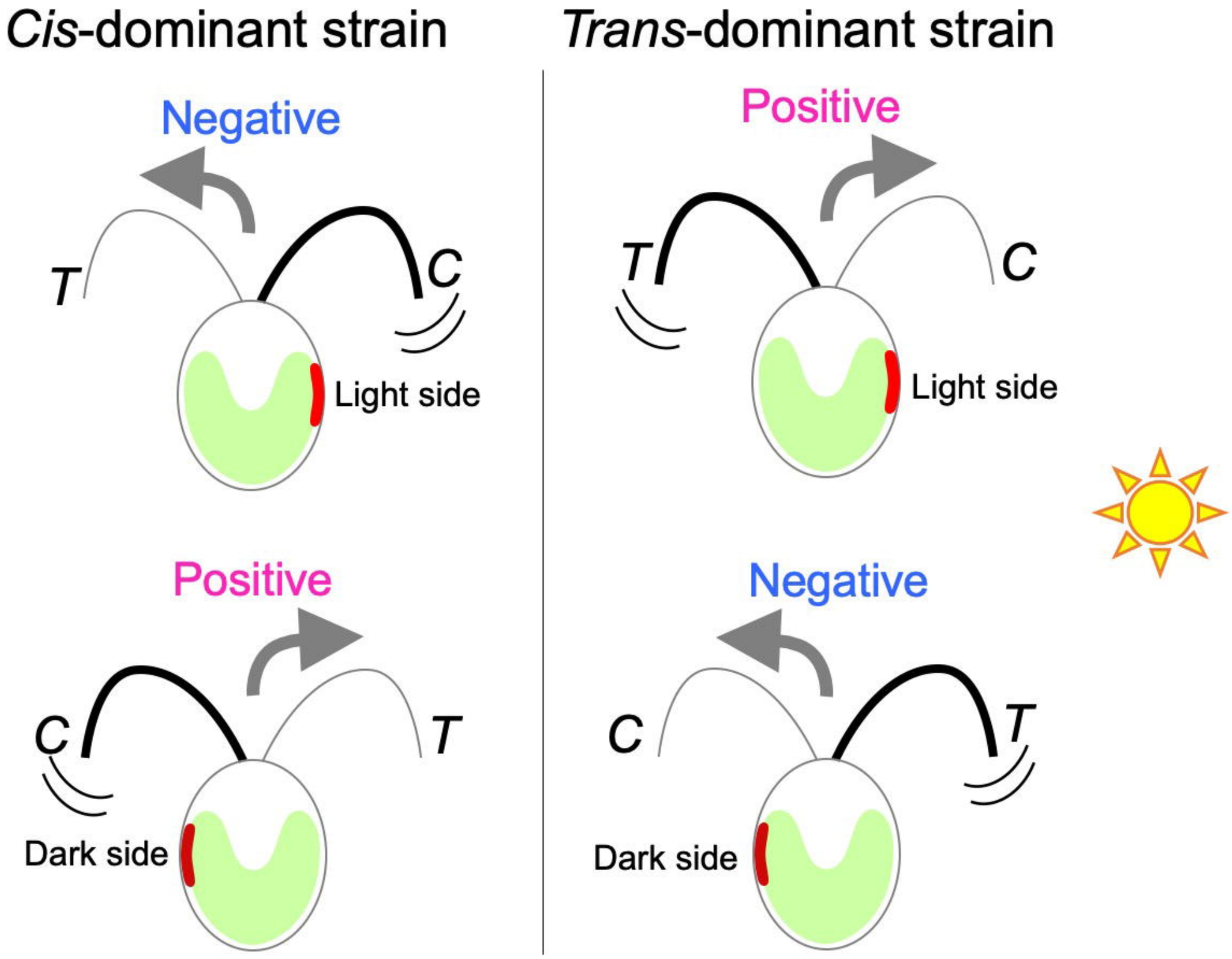

Fig. 8 **Schematic model of sign-reversal in phototaxis suggested by this study.**